DISCRETE AND CONTINUOUS
DYNAMICAL SYSTEMS–SERIES B
Volume **6**, Number **5**, September **2006**

Website: http://AIMsciences.org

pp. **979–1000**

LAGRANGIAN AVERAGING FOR THE $1D$ COMPRESSIBLE EULER EQUATIONS

Harish S. Bhat

Applied Physics and Applied Mathematics
Columbia University, New York NY 10027, USA

Razvan C. Fetecau

Department of Mathematics
Stanford University, Stanford CA 94305-2125 , USA

(Communicated by Doron Levy)

Abstract. We consider a 1-dimensional Lagrangian averaged model for an inviscid compressible fluid. As previously introduced in the literature, such equations are designed to model the effect of fluctuations upon the mean flow in compressible fluids. This paper presents a traveling wave analysis and a numerical study for such a model. The discussion is centered around two issues. One relates to the intriguing wave motions supported by this model. The other is the appropriateness of using Lagrangian-averaged models for compressible flow to approximate shock wave solutions of the compressible Euler equations.

1. **Introduction.** The purpose of this work is to perform a traveling wave analysis and a numerical study for a simplified version of one of the Lagrangian averaged compressible models considered in [11] and [2]. The equations introduced in [11] and [2] were designed to model the effect of fluctuations upon the mean flow in compressible fluids. The technique used in these papers to derive the mean motion equations is the so-called Lagrangian averaging approach. The distinctive feature of this approach, as compared to traditional filtering, is that averaging is carried out at the level of the variational principle and not at the level of the equations (in this case, Euler or Navier-Stokes equations). Examples of the latter approach are the Reynolds averaged Navier-Stokes (RANS) and the large eddy simulation (LES) models, both heavily used in computational fluid dynamics.

The Lagrangian averaged incompressible fluid models have received a good deal of attention since they first appeared in [13; 12]. They are known in the literature as Lagrangian averaged Euler (LAE-α) and Lagrangian averaged Navier-Stokes (LANS-α) equations. We refer the interested reader to [19] for a detailed history of the analysis for LAE-α and LANS-α equations and to [20] for a survey and further references about the numerical aspects of these models. In short, from an analytical viewpoint, the study of these models may shed light and provide insight on one of the most challenging open problems in applied analysis: the global well-posedness for 3-dimensional Euler and Navier-Stokes equations. For instance, the 3-dimensional

2000 *Mathematics Subject Classification.* 37K05, 76N99, 37N10.
Key words and phrases. Lagrangian averaging, compressible fluids.

LANS-α equations possess global regularity of solutions (see [9; 19]). From a computational viewpoint, the Lagrangian averaged incompressible fluid equations were successfully used as turbulence models (see [6; 20]).

As regards the compressible case and the Lagrangian averaged models introduced in [11] and [2], we note that these two papers present only derivations of the mean flow equations and do not perform any analytical or numerical studies of the models. Moreover, the n-dimensional model equations derived there are lengthy and involve high-order derivatives and inverse elliptic operators. For this reason, the author of [11] presents the 1-dimensional case separately and makes the remark (see page 256) that such 1-dimensional models "should provide ample opportunities for testing the dynamical effects of fluctuations on the one dimensional Lagrangian mean fluid motion, without requiring the more intensive numerics and analysis needed in higher dimensions."

In this paper we only consider a simplified 1-dimensional Lagrangian averaged compressible model. We believe, however, that the behavior of solutions of this 1-dimensional model is typical of most of the Lagrangian averaged compressible models presented in [11] and [2].

Examining 1-dimensional ($1D$) models will enable us to answer the following questions:

1. What types of wave motions are supported by Lagrangian-averaged models for compressible flow?
2. Can Lagrangian-averaged models for compressible flow be used to approximate shock wave solutions of the compressible Euler equations?

Let us first present the simplest possible $1D$ Lagrangian averaged model for barotropic compressible flow. Here ρ is the density, u is the velocity, $W(\rho)$ is the potential energy of a barotropic fluid and p denotes the pressure. We assume that the $p(\rho)$ is given by the state equation $p = \kappa\rho^\gamma$, which corresponds to a potential energy

$$W(\rho) = \frac{\kappa}{\gamma - 1}\rho^{\gamma-1}. \tag{1}$$

Also, we use the definition of v given by

$$v := u - \alpha^2 u_{xx}. \tag{2}$$

Our averaged model is derived from the Lagrangian

$$l = \int \left[\frac{1}{2}\left(\rho u^2 + \alpha^2 \rho u_x^2\right) - \rho W(\rho)\right] dx. \tag{3}$$

Here, α is a small positive number. In [2], α represents the coarseness of the average, for instance. The semidirect product Euler-Poincaré equations (see [12]) for this Lagrangian are

$$\rho_t + (\rho u)_x = 0, \tag{4a}$$

$$w_t + (uw)_x - \frac{1}{2}\left(u^2 + \alpha^2 u_x^2\right)_x = -\frac{p_x}{\rho}, \tag{4b}$$

where we define w via

$$\rho w := \rho v - \alpha^2 \rho_x u_x. \tag{5}$$

Using (5), we can show that (4b) is equivalent to the following equation for u only:

$$\rho u_t + \rho u u_x - \alpha^2\left(\rho_x u_{xt} + \rho_x u u_{xx} + \rho u_x u_{xx} + \rho u_{xxt} + \rho u u_{xxx}\right) = -p_x. \tag{6}$$

From now on, we shall refer to the system (4-5) or, equivalently, (4a) and (6), as System S.

The main analytical result of this work is contained in Theorem 1 and regards the existence of traveling waves for System S.

Remark. If we set $\alpha = 0$, the system (4) reduces to the compressible barotropic Euler equations. However, the behavior of solutions of (4) as $\alpha \to 0$ may be very subtle, as we will explain later.

Outline of this paper. In Section 2, we will motivate System S in a few different ways, showing how it can be derived from the full-blown models of [11] and [2] or from a simple filtering argument. Also, in Section 2 we derive the equations of motion using the semidirect product theory developed in [12]. Next, in Section 3, we describe various wave propagation properties of System S, including a large class of traveling wave solutions. In Section 4, we numerically study the initial-value problem for System S, with an eye towards checking its shock-approximation qualities. We list our conclusions and potential avenues for future work in Section 5.

Summary of results. Regarding the two questions posed above, we will show that:

1. System S supports intriguing wave phenomena and pattern formation, raising many questions of mathematical interest. Also, System S is, in a certain sense, a compressible generalization of a well-known dispersive wave equation.
2. System S does not approximate shock solutions of the compressible Euler equations. However, the wave solutions of System S indicate where/how we should look for a Lagrangian-averaged model for compressible flow that is capable of capturing shocks.

2. **Motivation and Derivation.**

2.1. **Motivation.** Let us explain how we arrived at the kinetic energy terms in the Lagrangian (3). It should be understood that the kinetic energy in (3) is a replacement for the usual compressible Euler kinetic energy, which is

$$\int \rho u^2 \, dx. \tag{7}$$

The potential energy term that we use,

$$\int \rho W(\rho) \, dx, \tag{8}$$

is precisely the potential energy for compressible Euler.

Compressible averaged Lagrangians previously considered in the literature. The Lagrangian (3) is a simplified version of the averaged Lagrangians introduced in [2] and [11].

Averaged Lagrangians derived in [2]. In [2], the authors derive a rather general form of an averaged Lagrangian for compressible flow. The averaging in that derivation took place over small-scale material-frame fluctuations. These fluctuations in the material picture induce fluctuations in the velocity u and the density ρ in the spatial picture. If we ignore the density fluctuations, then the final averaged Lagrangian in [2] (see equation (4.5) on page 829) reduces to

$$l(u,\rho) = \int \left\{ \frac{1}{2}\rho\|u\|^2 - \rho W(\rho) + \frac{\alpha^2}{2}\rho \left\langle \left\| \frac{D\xi'}{Dt} \right\|^2 \right\rangle \right\} dx, \tag{9}$$

where α represents the coarseness of the average, ξ' are material frame fluid fluctuations and D/Dt is the material derivative:

$$\frac{D}{Dt} = \partial_t + u \cdot \nabla.$$

If we now assume that the fluctuations ξ' are Lie-advected by the mean flow u and that the Lagrangian covariance tensor $\langle \xi' \otimes \xi' \rangle$ is the identity, i.e.,

$$\partial_t \xi' = -\pounds_u \xi',$$
$$\left\langle \xi'^j \xi'^k \right\rangle = \delta^{jk},$$

we will find that

$$\left\langle \left\| \frac{D\xi'}{Dt} \right\|^2 \right\rangle = u^i_{,j} u^i_{,k} \left\langle \xi'^j \xi'^k \right\rangle = \|\nabla u\|^2 .$$

Here, we adopted the convention of summation over repeated indices. Hence, the kinetic energy from (9) becomes

$$\int \frac{1}{2} \left(\rho \|u\|^2 + \alpha^2 \rho \|\nabla u\|^2 \right) dx.$$

Restricting to one spatial dimension yields the kinetic energy for System S.

Averaged Lagrangians derived in [11]. Using different formalism and an averaging procedure that differs from that of [2], D. D. Holm has derived in [11], the "1D Lagrangian and Eulerian mean polytropic gas equations" (see Section 11.2 and Section 13.3, respectively). Holm's potential energy is precisely the same as ours, and his kinetic energy is

$$\frac{1}{2} \int \rho \left(u^2 + w u_x^2 \right) dx,$$

where $w = \langle \xi' \xi' \rangle$ is the mean covariance of material frame fluctuations in one dimension. Our kinetic energy corresponds to taking this mean covariance to be constant and positive: $w = \alpha^2$. Holm derives the following evolution equation for w in the Eulerian mean model (see [11, Section 13.3]):

$$w_t + u w_x = 0.$$

Hence $w(x,t) = \alpha^2$ is the global unique solution corresponding to the initial data $w(x,0) = \alpha^2$. So $w = \alpha^2$ is in fact an invariant manifold of initial conditions for the general Eulerian mean model. Holm points this out and refers to our model as the "polytropic gas alpha model." No analysis of solutions of the model is carried out. An alternative derivation. In [11] and [2], the averaging is carried out over fluctuations in the material frame. We give below an alternative derivation of the Lagrangian (3), based on filtering in the spatial frame. Later we review an advantage of this approach.

Favré Filtering. The kinetic energy term for System S is

$$\frac{1}{2} \int \rho \left(u^2 + \alpha^2 u_x^2 \right) dx. \tag{10}$$

We arrive at this term by filtering (7) via a simple procedure that we shall now describe. Suppose there is a filter $f \mapsto \overline{f}$ which satisfies four basic properties:

P1. $\overline{af + bg} = a\overline{f} + b\overline{g}$ for scalar constants a and b,
P2. $\overline{\overline{f}} = \overline{f}$,
P3. $\overline{\overline{f} g} = \overline{f}\,\overline{g}$,

P4. $(\overline{f})_x = \overline{(f_x)}$ and $(\overline{u})_t = \overline{(u_t)}$.

Following [8] or [21], we define the Favré, or density-weighted, filter as follows:

$$f \mapsto \tilde{f} = \frac{\overline{\rho f}}{\overline{\rho}}. \tag{11}$$

The reader can easily verify that properties P1-P3 of the $f \mapsto \overline{f}$ filter are true for the Favré filter as well. Note that if we decompose $f = \overline{f} + f'$, we must have $\overline{f} = \overline{\overline{f}} + \overline{f'}$. Then property P2 forces $\overline{f'} = 0$. The same holds for the Favré filter.

Mass transport. One might ask why we use two different filters. With our setup, we filter the continuity equation and find

$$0 = \overline{\rho_t + (\rho u)_x} = \overline{\rho}_t + (\overline{\rho u})_x = \overline{\rho}_t + (\overline{\rho}\tilde{u})_x. \tag{12}$$

Therefore, the filtered variables $\overline{\rho}$ and $\tilde{u}$ satisfy the ordinary continuity equation. Note that if we define the volume form $\overline{\mu} = \overline{\rho}\, dx$, then we find that (12) implies

$$\frac{\partial \overline{\mu}}{\partial t} = -\pounds_{\tilde{u}} \overline{\mu}.$$

This means that if we define the filtered material motion $\tilde{\eta}$ by $\partial_t \tilde{\eta} = \tilde{u} \circ \tilde{\eta}$, the filtered material density will satisfy

$$\overline{\nu} = \tilde{\eta}_* \overline{\nu}_0,$$

where $\overline{\nu}(X,t) = \overline{\mu}(\tilde{\eta}(X,t),t)$ and $\overline{\nu}(X,0) = \overline{\nu}_0$. We conclude that Favré filtering respects standard mass transport in both the spatial and material frames. This is a desirable feature of the approach.

Filtered kinetic energy. Introducing the decomposition $u = \tilde{u} + u'$, we filter the kinetic energy (7):

$$\int \overline{\rho u^2}\, dx = \int \overline{\rho}\widetilde{u^2}\, dx = \int \overline{\rho} \left(\widetilde{\tilde{u}^2} + 2\widetilde{\tilde{u}u'} + \widetilde{u'^2} \right) dx. \tag{13}$$

Note that the cross-term $\widetilde{\tilde{u}u'}$ vanishes, by application of P3 and P2:

$$\widetilde{\tilde{u}u'} = \tilde{u}\widetilde{u'} = 0.$$

By applying P3 and P2 in the same way, we derive $\widetilde{\tilde{u}^2} = \tilde{u}^2$. Now we make one assumption:

$$\int \overline{\rho}\widetilde{u'^2}\, dx \approx \int \alpha^2 \overline{\rho} \tilde{u}_x^2\, dx. \tag{14}$$

Here α is a small parameter with units of length. Justification of (14) stems from three arguments:

1. The left-hand side of (14) is a weighted L^2 norm of the fluctuations u'. In order to produce a closed model, we must estimate this norm in terms of $\tilde{u}$ only. A reasonable candidate for the estimate is a measure of how wiggly $\tilde{u}$ is—and this is precisely the right-hand side of (14). We introduce α, a small parameter with units of length, as the effective filter width. That is, we want our estimate to respect the fact that as the filter becomes finer, i.e., as $\alpha \to 0$, less mass from u goes into u'. That is,

$$\int \overline{\rho}\widetilde{u'^2}\, dx \to 0 \quad \text{as} \quad \alpha \to 0.$$

2. Validation of (14) can be done using direct numerical simulations of $1D$ gas dynamics. Using various filters, we have found good agreement between both sides of (14), across a range of values of α. Note that in the averaging derivations of [11] and [2], the closure hypotheses involved the material fluctuations ξ' and are therefore difficult to verify numerically.
3. If we carry out the same filtering procedure in the incompressible regime, we will find that the modeling assumption

$$\int \|u'\|^2 \, \mathrm{d}^n x \approx \int \alpha^2 \|\nabla u\|^2 \, \mathrm{d}^n x.$$

yields the H^1 kinetic energy found in LAE-α models.

Putting all of this together, we see that (13) becomes

$$\int \overline{\rho u^2} \, dx \approx \int \overline{\rho} \tilde{u}^2 + \alpha^2 \overline{\rho} \tilde{u}_x^2 \, dx. \tag{15}$$

2.2. **Equations of Motion.** We regard the Lagrangian (3) as a functions of the vector field u and the volume form $\mu = \rho \, dx$. The equations of motions corresponding to these Lagrangians are the semidirect product Euler-Poincaré equations:

$$\frac{\partial}{\partial t} \frac{\delta l}{\delta u} = - \operatorname{ad}_u^* \frac{\delta l}{\delta u} + \frac{\delta l}{\delta \mu} \diamond \mu. \tag{16}$$

For a detailed derivation of these equations of motion and general definitions of all the terms involved, we refer to [12]. In the case we consider, where all functions, fields, and forms are defined over a one-dimensional manifold, we only need the following simplified forms of the ad^* and $\diamond$ operators. For a $1-$form θ and a vector field u, we have

$$\begin{aligned} \operatorname{ad}_u^*(\theta \otimes dx) &= (\pounds_u \theta + \theta \operatorname{div} u) \otimes dx \\ &= (\mathbf{d} \mathbf{i}_u \theta + \mathbf{i}_u \mathbf{d} \theta + u_x \theta) \otimes dx \\ &= (\mathbf{d} \mathbf{i}_u \theta + u_x \theta) \otimes dx. \end{aligned} \tag{17}$$

Also, for a scalar function f and a $1-$form μ, we have

$$f \diamond \mu = \mathbf{d} f \otimes \mu. \tag{18}$$

We compute the variational derivatives $\delta l / \delta u$ and $\delta l / \delta \mu$ for the Lagrangian (3), and then use these expressions in (16).

Derivation of System S.. We begin computing the Euler-Poincaré equations for the Lagrangian (3). The computations lead to

$$\frac{\delta l}{\delta u} = \left(\rho u - \alpha^2 \rho u_{xx} - \alpha^2 \rho_x u_x \right) dx \otimes dx. \tag{19}$$

The quantity inside parentheses is actually the momentum for System S, which we denote

$$\rho w = \rho v - \alpha^2 \rho_x u_x, \tag{20}$$

where v was defined in (2). Using (20), the formula (19) becomes

$$\frac{\delta l}{\delta u} = \rho w \, dx \otimes dx. \tag{21}$$

By applying formula (17) to (21), we get:

$$\operatorname{ad}_u^* \frac{\delta l}{\delta u} = \left[(\rho u w)_x + \rho u_x w \right] dx \otimes dx. \tag{22}$$

The computation of $\delta l/\delta\mu$ gives

$$\frac{\delta l}{\delta \mu} = \frac{1}{2}\left(u^2 + \alpha^2 u_x^2\right) - s(\rho), \tag{23}$$

where $s(\rho)$ is the enthalpy, defined by

$$s(\rho) = W(\rho) + \rho W'(\rho). \tag{24}$$

We introduce the pressure function p using

$$s_x = \frac{p_x}{\rho}. \tag{25}$$

By using (18) and (25) we can write

$$\frac{\delta l}{\delta \mu} \diamond \mu = \left[\frac{1}{2}\rho\left(u^2 + \alpha^2 u_x^2\right)_x - p_x\right] dx \otimes dx. \tag{26}$$

Plugging (21), (22) and (26) into (16) we obtain the momentum equation for System S:

$$\frac{\partial}{\partial t}(\rho w) + (\rho u w)_x + \rho u_x w - \frac{1}{2}\rho(u^2 + \alpha^2 u_x^2)_x = -p_x, \tag{27}$$

where ρw is given by (20). We also recall that the semidirect product theory treats the volume form $\rho\, dx$ as an advected quantity. This assumption leads to the continuity equation:

$$\frac{\partial \rho}{\partial t} + (\rho u)_x = 0. \tag{28}$$

By combining (27) and (28) we can derive:

$$w_t + (uw)_x - \frac{1}{2}\left(u^2 + \alpha^2 u_x^2\right)_x = -\frac{p_x}{\rho}. \tag{29}$$

In terms of u, the pde (29) reads

$$\rho u_t + \rho u u_x - \alpha^2\left(\rho_x u_{xt} + \rho_x u u_{xx} + \rho u_x u_{xx} + \rho u_{xxt} + \rho u u_{xxx}\right) = -p_x. \tag{30}$$

Conserved Energy. The Lagrangian (3) is of the form $K - V$, where K and V stand for kinetic and potential energy, respectively. As one might expect, the system conserves an energy of the form $K + V$. In fact, more is true. We state without proof that starting from the Hamiltonian

$$h = \int \left[\frac{1}{2}\left(\rho u^2 + \alpha^2 \rho u_x^2\right) + \rho W(\rho)\right] dx, \tag{31}$$

one may apply the semidirect product Lie-Poisson equations (see [18]) to derive System S. Since h contains no explicit time-dependence, we have by Noether's theorem the easy consequence that h is conserved in time along solutions of System S. Because we are dealing with an infinite-dimensional Hamiltonian system, this energy conservation is purely formal. To make the argument rigorous, we would have to prove that the initial-value problem for System S is well-posed in a function space such that $h(t) < \infty$ for all $t \geq 0$. We leave that as an open question; for our purposes, when we solve System S numerically, we expect the energy h should be conserved as long as the solution remains smooth.

3. **Traveling Waves.** Typically, one searches for traveling wave solutions by way of the ansatz

$$u = u\left(\frac{x-ct}{\alpha}\right) \quad \text{and} \quad \rho = \rho\left(\frac{x-ct}{\alpha}\right). \tag{32}$$

However, System S is Galilean invariant. By this we mean that the equations (4a) and (6) are unchanged by the transformation

$$\tilde{x} \mapsto x + u_0 t$$
$$\tilde{u} \mapsto u + u_0,$$

for any $u_0 \in \mathbb{R}$. This implies that if the system has traveling wave solutions $u(x-ct)$ for some fixed $c = c_0$, then it has solutions for all c. Hence for System S it is sufficient to consider $c = 0$, so we take the ansatz

$$u = u(x/\alpha) \quad \text{and} \quad \rho = \rho(x/\alpha). \tag{33}$$

This traveling wave form includes a factor of α^{-1} in the argument, which we shall see eliminates α from the resulting traveling wave ode. In what follows, the primes represent differentiation with respect to the variable $z = x/\alpha$.

Continuity equation. We start with (4a) and introduce the ansatz (33), resulting in

$$u\rho' + \rho u' = 0,$$

or

$$\rho'/\rho = -u'/u. \tag{34}$$

This can be trivially integrated, and the answer is

$$\rho = B/u, \tag{35}$$

for an arbitrary constant B.

Momentum equation. Next we consider (4b), with pressure term given by $p = \kappa\rho^\gamma$. Using the ansatz (33) and equation (34) in (5), we find that w is related to u by

$$w = u - u'' + \frac{u'^2}{u}. \tag{36}$$

The barotropic state equation becomes

$$\frac{p'}{\rho} = \kappa\gamma\rho^{\gamma-2}\rho'. \tag{37}$$

Using (34-37) in equation (4b), we can derive

$$u' - u''' = \kappa\gamma B^{\gamma-1}u^{-\gamma-1}u'. \tag{38}$$

Trivially integrating both sides, we obtain

$$u'' = u + \kappa B^{\gamma-1}u^{-\gamma} - C_1, \tag{39}$$

where $C_1 \in \mathbb{R}$ is an arbitrary constant. As this is a single second-order equation, we may choose values for the various constants and plot the phase portrait numerically—see Figure 1 for the specific case $\kappa = 0.4$, $\gamma = 1.4$, $B = 1$, $C_1 = 2$. The phase portrait features two fixed points marked by filled circles. The left fixed point is clearly a nonlinear center surrounded by periodic orbits. The right fixed point is a saddle with a homoclinic orbit marked by arrows. Note that the only trajectories that remain bounded as $z \to \pm\infty$ are the homoclinic orbit and the periodic orbits contained inside.

There is a line of essential singularities at $u = 0$. Existence and uniqueness of solutions hold for initial conditions in the set $\{(u, u') \in \mathbb{R}^2 \text{ s.t. } u \neq 0\}$, including points arbitrarily close to $u = 0$. However, it is possible for two or more different

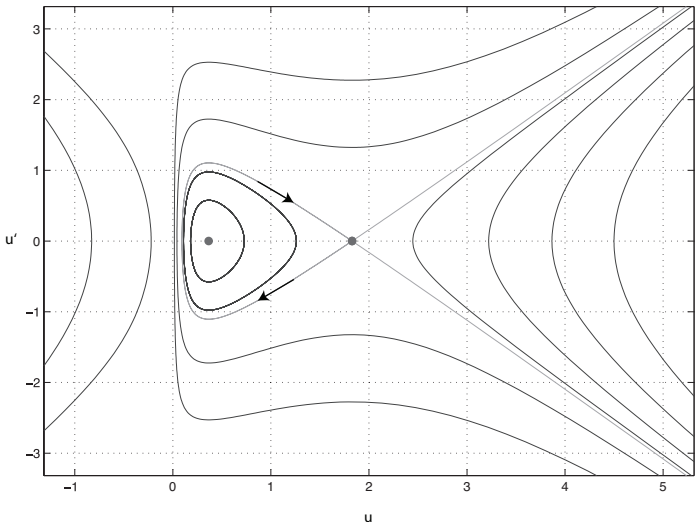

FIGURE 1. Sample phase portrait u vs. u' for ode (39), with $\kappa = 0.4$, $\gamma = 1.4$, $B = 1$, $C_1 = 2$.

trajectories to have α- or ω-limit sets[1] consisting of the same point on the line $u = 0$.

Now let us attempt to show that the general phase portrait of (39) resembles what we saw numerically in Figure 1.

It is obvious that (39) is Hamiltonian. Let $K(u') = {u'}^2/2$ denote the kinetic energy; then, with the potential energy

$$V(u) = -\frac{1}{2}u^2 + C_1 u + \frac{\kappa B^{\gamma-1}}{\gamma - 1}u^{1-\gamma}, \tag{40}$$

we may write the Hamiltonian for (39) as

$$H(u, u') = K(u') + V(u). \tag{41}$$

Note: for $\gamma = 1$, the potential $V(u)$ must be modified, as must the following discussion. We tacitly assume $\gamma \neq 1$ in what follows. Continuing, the fixed-energy level set $H(u, u') = C_2$ is given by the locus of points (u, u') that satisfy

$$\frac{1}{2}{u'}^2 - \frac{1}{2}u^2 + C_1 u + \frac{\kappa B^{\gamma-1}}{\gamma - 1}u^{1-\gamma} = C_2. \tag{42}$$

The equilibria of (39) are the extrema of V. Hence we search for zeros of

$$V'(u) = -u + C_1 - \kappa B^{\gamma-1}u^{-\gamma}. \tag{43}$$

Let us keep in mind that C_1, C_2, and B are constants that appear in the ode only—they do not appear anywhere in System S, as is obvious from (4). By adjusting the values of these parameters, one can obtain an infinite number of traveling wave solutions for System S. To show this, we first prove

Lemma 1. *Given any pair of distinct reals u_1, u_2 with the same sign, there exist B and C_1 such that $V'(u_1) = V'(u_2) = 0$. This is true for all $\kappa, \gamma > 0$.*

[1]Here we mean α- and ω-limit sets in the dynamical systems sense (see [1]). There is no connection between this and the α that we use elsewhere.

Proof. Regard u_1, u_2, κ, and γ as given and solve the system

$$-u_1 + C_1 - \kappa B^{\gamma-1} u_1^{-\gamma} = 0$$
$$-u_2 + C_1 - \kappa B^{\gamma-1} u_2^{-\gamma} = 0$$

for B and C_1. One finds that

$$B = \left[\frac{1}{\kappa}\left(\frac{u_2 - u_1}{u_2^\gamma - u_1^\gamma}\right)(u_1 u_2)^\gamma\right]^{1/(\gamma-1)}$$
$$C_1 = \frac{u_1^{1+\gamma} - u_2^{1+\gamma}}{u_1^\gamma - u_2^\gamma}.$$

C_1 is well-defined since $u_1 \neq u_2$. Because u_1 and u_2 have the same sign, for all $\kappa, \gamma > 0$, the argument inside square brackets in the expression for B is always positive. Hence we may always raise this argument to the $1/(\gamma-1)$ power, so B is well-defined. □

Now that we have established that the equilibria of (39) may be arbitrarily chosen, we should examine their stability.

Lemma 2. *Suppose u_1, u_2 satisfy the hypotheses of Lemma 1, and suppose $|u_1| < |u_2|$. Then u_1 is stable and u_2 is unstable for all $\kappa, \gamma > 0$.*

Proof. First suppose $0 < u_1 < u_2$. Differentiating (43), we have

$$V''(u) = -1 + \kappa\gamma B^{\gamma-1} u^{-\gamma-1}. \tag{44}$$

We evaluate this at $u = u_1$ and $u = u_2$ and use the formula for B given by Lemma 1 to obtain

$$V''(u_1) = -1 + \gamma \frac{u_2}{u_1} \frac{1 - (u_1/u_2)}{1 - (u_1/u_2)^\gamma} \tag{45a}$$

$$V''(u_2) = -1 + \gamma \frac{u_1}{u_2} \frac{1 - (u_2/u_1)}{1 - (u_2/u_1)^\gamma}. \tag{45b}$$

The signs of (45a-45b) are determined by the behavior of the function

$$f(x) = -1 + \frac{\gamma}{x} \frac{1 - x}{1 - x^\gamma}. \tag{46}$$

Let us list some facts about f that can be shown using elementary calculus:

$$\lim_{x\to 0} f(x) = +\infty,$$
$$\lim_{x\to 1} f(x) = 0,$$
$$\lim_{x\to +\infty} f(x) = -1,$$
$$f'(x_0) = 0 \iff 1 + \gamma(1 - x_0) = x_0^{-\gamma},$$
$$f'(x_0) = 0 \implies f''(x_0) < 0.$$

It is impossible for a function to have *only* local maxima while decreasing from $+\infty$ to zero, and then from zero to -1. Hence f does not have any critical points on $(0, \infty)$, implying $f'(x) < 0$ for all $x > 0$. Now we return to (45a-45b). Because u_1 and u_2 have the same sign,

$$\frac{|u_1|}{|u_2|} = \frac{u_1}{u_2}.$$

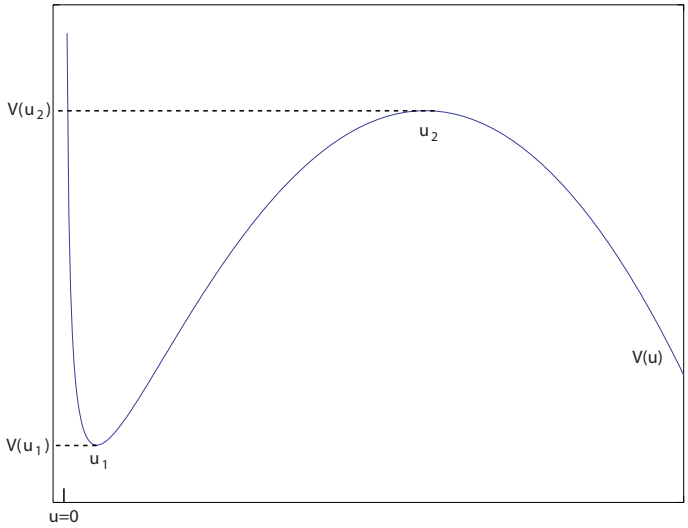

FIGURE 2. Potential energy for the Hamiltonian ode (39).

As $|u_1|/|u_2| < 1$ and $f(x) > 0$ for $x < 1$, we have $V''(u_1) > 0$, so u_1 is stable. Similarly, since $f(x) < 0$ for $x > 1$ and $|u_2|/|u_1| > 1$, we have $V''(u_2) < 0$, so u_2 is unstable. □

Using Lemmas 1 and 2, for any $\kappa, \gamma > 0$, and for any u_1, u_2 satisfying $0 < u_1 < u_2$, we may fix various constants so that the potential energy V is as shown in Figure 2. To answer the question of what happens when we choose $u_2 < u_1 < 0$, an inspection of the potential (40) reveals that we must specify γ, at least in the exponent of u. The constant γ in the barotropic state law is the ratio of specific heats for the compressible fluid. For an ideal gas, we may derive (see [23]) the relationship $\gamma = 1 + 2/n$, where n is the total number of degrees of freedom for each gas molecule. With this in mind, it is clear that $1 - \gamma = -2/n$ and hence the potential V is invariant under the reflection $u \mapsto -u$, $C_1 \mapsto -C_1$. Then V satisfies

$$\lim_{u \to 0} V(u) = +\infty$$
$$\lim_{u \to \pm\infty} V(u) = -\infty,$$

and the behavior of V for $u < 0$ is given by the reflection of Figure 2 across the $u = 0$ line.

For the purposes of solving the System S pde, we are interested in solutions $u(z)$ of the ode (39) that stay bounded as $z \to \pm\infty$. From the above description of the potential together with the energy integral (42), it is clear that such solutions exist when

$$V(u_1) \leq C_2 \leq V(u_2).$$

Indeed, if we set $C_2 = V(u_2)$, we find that the solution of

$$\frac{1}{2}u'^2 = V(u_2) - V(u)$$

is the homoclinic orbit for the fixed point $(u, u') = (u_2, 0)$. Taking C_2 such that $V(u_1) < C_2 < V(u_2)$, we find that (42) describes periodic trajectories of the system. Let us quickly summarize this result:

Lemma 3. *Let $\kappa > 0$ be arbitrary and let $\gamma = 1 + 2/n$ for some positive integer n. Given any u_1, u_2 of the same sign, we may choose B and C_1 such that the Hamiltonian ode (39) has a homoclinic orbit $u(z)$ that connects the u_2 equilibrium with itself. The solution $u(z)$ is a real-analytic function of z.*

Proof. Without loss of generality, suppose $|u_1| < |u_2|$. Examine Figure 2 and denote by u^* the first point of intersection of the upper dashed line with the blue $V(u)$ curve. That is, define u^* such that $|u^*| < |u_1|$ and

$$V(u^*) = V(u_2).$$

Imagine a fictitious particle situated on the graph, that starts from rest at the point $(u^*, V(u_2))$. This particle will reach $(u_2, V(u_2))$ in an infinite amount of "time." That is, the trajectory $(u(z), u'(z))$ that emanates from $(u(0), u'(0)) = (u^*, 0)$ satisfies

$$\lim_{z\to\pm\infty} u(z) = u_2$$
$$\lim_{z\to\pm\infty} u'(z) = 0.$$

This is the homoclinic trajectory in question, connecting the fixed point $(u_2, 0)$ to itself. Note that we may force $|u^*|$ to be as small as we want by choosing $|u_1|$ sufficiently small. That the solution $u(z)$ is real-analytic follows[2] from the fact that the right-hand side of (39) is a real-analytic function of u away from the singularity line $u = 0$. □

Solving the pde. The technique of finding traveling wave solutions of a pde by searching for homoclinic orbits of an associated ode can be found in Chapter 3 of [17]. In our case, the analogy is trivial, because the homoclinic solutions $u(z)$ of the Hamiltonian ode (39) are related to solutions of the System S pde by the ansatz (32).

Because of Galilean invariance, we investigated only the $c = 0$ case of this ansatz. For arbitrary c, it is a simple matter to see that (39) would now possess a line of singularities at $u = c$ instead of at $u = 0$. Adjusting the results accordingly, we arrive at the following:

Theorem 1. *Let $\alpha > 0$ and $c \in \mathbb{R}$ be arbitrary. Let $\kappa > 0$ be arbitrary and let $\gamma = 1+2/n$ for some positive integer n. Given any u_1, u_2 such that $u_1 - c$ and $u_2 - c$ have the same sign, the System S pde (4) considered on the domain $(x, t) \in \mathbb{R} \times \mathbb{R}$ has either of two possible traveling wave solutions.*

1. *In case $u_2 > u_1 > c$, we have the* depression *wave solution $u(x, t), \rho(x, t)$ such that*

$$\lim_{x\to\pm\infty} u(x, t) = u_2,$$
$$u(ct, t) = u^*,$$
$$\rho(x, t) = \frac{B}{u(x, t) - c},$$

where $c < u^* < u_1$.

[2]For a proof that a real-analytic vector field possesses real-analytic integral curves, see [3, Chap. 6.10].

2. *In case $u_2 < u_1 < c$, we have the* elevation *wave solution $u(x,t)$ such that*

$$\lim_{x\to\pm\infty} u(x,t) = u_2,$$
$$u(ct,t) = u^*,$$
$$\rho(x,t) = \frac{-B}{u(x,t)-c},$$

where $u_1 < u^* < c$.

Proof. In what follows, we label the points such that $c < |u_1| < |u_2|$. As all the constants in the theorem satisfy the conditions of Lemmas 1, 2, and 3, we may solve the Hamiltonian ode (39) for a homoclinic orbit $u^0(z)$ that connects u_2 to itself. We take[3]

$$\rho^0(z) = \frac{\pm B}{u^0(z)-c},$$

and choose either the plus sign if $u(z) > c$ or the minus sign if $u^0(z) < c$. The solution then satisfies $\rho^0 > 0$ everywhere. Now it is clear from the ansatz (33) that the functions

$$u(x,t) = u^0\left((x-ct)/\alpha\right),$$
$$\rho(x,t) = \rho^0\left((x-ct)/\alpha\right)$$

satisfy System S for all x and all t. Then we may compute the movement of the trough/peak of the wave:

$$u(ct,t) = u^0(0) = u^*$$

as in Lemma 3. □

Boundary conditions. *Finite domain.* Let us reconsider System S on the finite domain $x \in [0, L]$, and impose periodic boundary conditions:

$$u(0,t) = u(L,t), \tag{47a}$$
$$\rho(0,t) = \rho(L,t), \tag{47b}$$

for all times t.

Now when we examine the traveling wave ode (39), we must search for periodic solutions. However, it is already clear from Figure 2 that there are an infinite number of periodic solutions. Just imagine a fictitious particle starting from rest at any point on the $V(u)$ curve strictly between the dashed lines $V(u_1)$ and $V(u_2)$. The particle will oscillate (forever) inside the potential well with some period $L < \infty$. As we did before, we can use this periodic solution of the ode and the ansatz (33) to generate a traveling wave solution of System S, now posed with periodic boundary conditions (47).

Note that on the periodic interval, all traveling wave solutions have bounded energy (31).

Infinite domain. Let us now investigate appropriate boundary conditions on System S that render finite the energy (31) for solutions given by Theorem 1. For such solutions, $u \to u_2$ and

$$\rho \to \rho_2 := \frac{\pm B}{u_2 - c}$$

[3]Note that the constant B entered the ode analysis only through its $\gamma - 1$ power. Since $\gamma - 1 = 2/n$, none of the ode results change if we replace B with $-B$.

as $x \to \pm\infty$. Here the sign of B is chosen so that $\rho_2 > 0$. As $u_2 \neq c$, it is clear that $0 < \rho_2 < \infty$. Hence the potential energy

$$\int \rho W(\rho)\, dx,$$

with W given in (1), cannot be finite for any traveling wave solution. However, there are traveling wave solutions that keep the kinetic energy (10) finite. These correspond to the case where $u \to 0$ sufficiently rapidly as $x \to \pm\infty$.

Dispersion relation. For any wave equation, knowledge of the dispersion relation $\omega(k)$ is quite important. If $\omega(k)$ is linear in k, then both the phase and group velocities are constant with respect to k, implying that waves of different wave number all propagate at the same speed. In such a case, we refer to the dynamics as *hyperbolic*. If $\omega(k)$ is nonlinear in k, then waves of different wave number propagate at different speeds. As time increases, a packet consisting of a superposition of different wavenumbers will therefore disperse, or spread out, in space. In this case, we refer to the dynamics as *dispersive*.

With this terminology, now widely used but originally due to Whitham (see [24]), the $1D$ barotropic compressible Euler equation is a nonlinear hyperbolic equation. Typical behavior in such a system is steepening of wave profiles and the formation of sharp discontinuities, or shock waves. As we have seen, System S has a large family of solitary wave solutions, which is typical of nonlinear dispersive equations such as the Korteweg-de Vries (KdV), Nonlinear Schrödinger (NLS), and sine-Gordon equations. As we shall now see, System S is indeed a dispersive system, but this is not the full story.

In order to compute the dispersion relation for System S, we shall have to deal with both the continuity equation (4a) and the velocity equation (6). The first equation is unchanged from the compressible Euler context, and therefore retains its hyperbolic character. Indeed, linearizing (4a) about a constant solution[4] via

$$\rho(x,t) = \rho_0 + \varepsilon \exp i(kx - \omega t), \tag{48}$$

$$u(x,t) = u_0 + \varepsilon \exp i(kx - \omega t), \tag{49}$$

we will obtain, at first-order in ε, the linear dispersion relation

$$\omega(k) = (u_0 + \rho_0)k.$$

This is the standard approach for obtaining dispersion relations, but it simply does not work for System S. The reason is that System S consists of a coupled hyperbolic-dispersive system. If we use the naïve approach of (48) and (49) in both the hyperbolic part (4a) and the dispersive part (6), we will not produce anything meaningful.

Therefore, we generalize the usual procedure. We retain the usual expression (49) for u consisting of a small sinusoidal perturbation from a constant state. Note that this is a traveling wave solution, with phase velocity $c = \omega/k$, so we expect from our earlier analysis that $\rho(x,t)$ will take the form

$$\rho(x,t) = \frac{B}{u(x,t) - \omega/k}, \tag{50}$$

for some constant B to be specified later. For now, we assume the existence of δ such that

$$u_0 - \frac{\omega}{k} = \delta = O(\varepsilon^0) \gg \varepsilon. \tag{51}$$

[4]The reader will verify by inspection that System S possesses the constant solution $\rho(x,t) = \rho_0$ and $u(x,t) = u_0$.

Later we shall determine a closed-form expression for δ. Now we must check that (49-50) solves the continuity equation (4a). We compute

$$\rho_x = -\frac{B\varepsilon ik \exp i(kx-\omega t)}{(u-\omega/k)^2}, \tag{52}$$

$$\rho_t = \frac{B\varepsilon i\omega \exp i(kx-\omega t)}{(u-\omega/k)^2}, \tag{53}$$

$$u_x = \varepsilon ik \exp i(kx-\omega t), \tag{54}$$

and the reader may verify that using this together with (49-50), we have

$$\rho_t + \rho_x u + \rho u_x = 0.$$

Hence we move on to the velocity equation (6), which we write as follows:

$$u_t + uu_x - \alpha^2\left(\frac{\rho_x}{\rho}\left(u_{xt}+uu_{xx}\right) + u_x u_{xx} + u_{xxt} + uu_{xxx}\right) = -\frac{p_x}{\rho}. \tag{55}$$

We are interested in the $O(\varepsilon)$ terms from (55). First let us put (49) together with (51) to get

$$u - \frac{\omega}{k} = \delta + O(\varepsilon) = O(\varepsilon^0). \tag{56}$$

At this point, it is clear that $u_x, u_{xx} = O(\varepsilon)$ and that

$$\frac{\rho_x}{\rho} = -\frac{u_x}{u-\omega/k} = \frac{O(\varepsilon)}{O(\varepsilon^0)} = O(\varepsilon).$$

Already we may eliminate three $O(\varepsilon^2)$ terms from (55) and rewrite it as

$$u_t + uu_x - \alpha^2\left(u_{xxt} + uu_{xxx}\right) = -\frac{p_x}{\rho}. \tag{57}$$

Now we choose the scalings $B = O(\varepsilon)$ and $\kappa = O(\varepsilon^{1-\gamma})$ in order to achieve the following balance:

$$\rho = \frac{B}{u-\omega/k} = O(\varepsilon),$$
$$p = \kappa\rho^\gamma = O(\varepsilon),$$
$$\frac{p_x}{\rho} = \kappa\gamma\rho^{\gamma-1}\frac{\rho_x}{\rho} = O(\varepsilon).$$

Hence all terms from (57) are $O(\varepsilon)$, so we may proceed to compute the dispersion relation. Note that from (56) we have

$$\frac{1}{u-\omega/k} = \frac{1}{\delta + O(\varepsilon)} = \frac{1}{\delta} + O(\varepsilon),$$

and raising both sides to the γ power, we obtain

$$(u-\omega/k)^{-\gamma} = \delta^{-\gamma},$$

where we are ignoring a term of order $O(\varepsilon^\gamma)$. In light of this, we may compute p_x/ρ:

$$\frac{p_x}{\rho} = -\kappa\gamma B^{\gamma-1}\delta^{-\gamma}\varepsilon ik \exp i(kx-\omega t).$$

Remembering that the right-hand side of (57) has a minus sign, we obtain, after substitution of our p_x/ρ result and (49),

$$-\omega(1+\alpha^2k^2) + u_0k(1+\alpha^2k^2) = \kappa\gamma B^{\gamma-1}\delta^{-\gamma}k.$$

This leads to

$$\omega(k) = u_0 k - \kappa\gamma B^{\gamma-1}\delta^{-\gamma}\frac{k}{1+\alpha^2k^2}.$$

Now we may attempt to "back out" an expression for δ. Let us compute

$$\delta = u_0 - \frac{\omega}{k} = \kappa\gamma B^{\gamma-1}\delta^{-\gamma}(1+\alpha^2k^2)^{-1}.$$

With δ in hand, we may write the dispersion relation for System S:

$$\omega(k) = u_0 k - \left(\frac{\kappa\gamma B^{\gamma-1}}{1+\alpha^2k^2}\right)^{1/(\gamma+1)} k. \tag{58}$$

Camassa-Holm. Interestingly, the dispersion relation for System S bears a resemblance to that of the Camassa-Holm equation:

$$v_t + uv_x + 2vu_x = 0, \tag{59a}$$

$$u - \alpha^2 u_{xx} = v. \tag{59b}$$

This equation was originally derived in [5] by vertically averaging the Hamiltonian for shallow water waves. Equation (59) is a completely integrable equation with a bi-Hamiltonian structure. Its geometric and analytical properties have been extensively studied. To compute its dispersion relation, we follow the usual procedure of taking sinusoidal perturbations about a constant solution as in (49). We obtain

$$\omega(k) = u_0 k + \frac{2u_0 k}{1+\alpha^2k^2}. \tag{60}$$

Also note that the Camassa-Holm equation (59) is the Euler-Poincaré equation for the Lagrangian

$$l(u) = \int u^2 + \alpha^2 u_x^2\, dx.$$

Comparing this with the System S Lagrangian (3), we see that both in terms of geometry and wave dynamics, System S can be considered a "compressible" version of Camassa-Holm.

Zero-α limit of solutions. It is clear from the dispersion relation (58) that α is not only a length scale that arises in the filtering/averaging derivation, but also a measure of dispersion in the model. For $\alpha > 0$, the dispersion relation $\omega(k)$ for System S depends nonlinearly on k. System S, or more specifically the momentum equation (6), is a dispersive regularization of the $1D$ barotropic compressible Euler equation.

Suppose we solve System S, on either the real line or a periodic interval, with initial data $\rho(x,0) = \rho_0$ and $u(x,0) = u_0$. Let us explicitly label the α-dependence of the resulting solution by writing it as $u^\alpha(x,t)$, $\rho^\alpha(x,t)$. The next question to ask is: what happens to these solutions as $\alpha \to 0$, or in other words, how do solutions of System behave in the zero-dispersion limit?

Let us take a slight digression and discuss the zero-dispersion limit of the Korteweg-de Vries (KdV) equation:

$$\begin{aligned} u_t + uu_x + \epsilon u_{xxx} &= 0, \\ u(x,0) &= u_0(x). \end{aligned} \tag{61}$$

The zero-ϵ limits of solutions of this equation is a zero-dispersion limit, and it has been pursued quite vigorously in the literature (see [16]). It is trivial to take $\epsilon \to 0$

in the KdV equation itself, and one obtains the (inviscid) Burgers equation

$$\begin{aligned} u_t + uu_x &= 0, \\ u(x,0) &= u_0(x). \end{aligned} \tag{62}$$

Taking $\epsilon \to 0$ in the *solutions* of the KdV equation is a completely different matter. The basic idea is that globally in time, as $\epsilon \to 0$, the solutions $u^\epsilon(x,t)$ of (61) equations do *not* converge to solutions of the limiting equation, which is (62). There is, of course, much more to the story than that:

- Assuming that $u_0(x)$ contains at least one point x_0 at which $u_0'(x) < 0$, the resulting solution $u(x,t)$ of (62) will develop a discontinuity in finite time. This happens regardless of how smooth $u_0(x)$ is. Let T denote the earliest time at which the solution $u(x,t)$ breaks—we refer to T as the *break time*.
- Now, for $t < T$, solutions $u^\epsilon(x,t)$ of the KdV equation (61) converge strongly to solutions $u(x,t)$ of the Burgers equation (62) with the same initial data.
- However, for $t > T$, solutions $u^\epsilon(x,t)$ of the KdV equation do not converge in *any* sense to weak solutions $u(x,t)$ of the Burgers equation. The solution $u^\epsilon(x,t)$ becomes highly oscillatory as ϵ vanishes—these oscillations are bounded in L^∞ but their frequency increases. In fact, it can be shown that $u^\epsilon(x,t)$ converges weakly to a solution of the Whitham modulation equation for KdV, which is quite different from the Burgers equation.

The above results summarize the content of the series of papers by Lax and Levermore [16] on the zero-dispersion limit of the KdV equation. The zero-dispersion limit of KdV has been framed as a Riemann-Hilbert problem [7], and the Riemann-Hilbert approach has been used (see [15] and [22]) to analyze the semiclassical, or zero-dispersion, limit of the NLS equation:

$$\begin{aligned} i\epsilon u_t + \frac{1}{2}\epsilon^2 u_{xx} + |u|^2 u &= 0, \\ u(x,0) &= u_0(x). \end{aligned} \tag{63}$$

Qualitatively identical phenomena, including high-frequency oscillations and weak limits, have been discovered in this case.

It is reasonable to conclude that analyzing the zero-α limit of System S is most likely a subtle and mathematically challenging problem. Furthermore, it seems unlikely that, as $\alpha \to 0$, we can extract information about gas dynamics from the solution $u^\alpha(x,t)$, $\rho^\alpha(x,t)$ of System S. That is, even if u^α and ρ^α converge to some functions as $\alpha \to 0$, this convergence is likely to be weak, and the limit functions are not likely to be solutions of the $1D$ barotropic compressible Euler equations.

4. **Initial-value Problem: Numerics.** We wish to study not only the traveling wave solutions of System S, but also the general initial-value problem for unknown functions $\rho : U \times [0,\infty) \to \mathbb{R}$ and $u : U \times [0,\infty) \to \mathbb{R}$:

$$\rho_t + (\rho u)_x = 0, \tag{64a}$$

$$\rho u_t + \rho u u_x - \alpha^2 \left(\rho_x u_{xt} + \rho_x u u_{xx} + \rho u_x u_{xx} + \rho u_{xxt} + \rho u u_{xxx}\right) = -p_x, \tag{64b}$$

$$\rho(x,0) = \rho_0(x), \tag{64c}$$

$$u(x,0) = u_0(x). \tag{64d}$$

Here, $U \subset \mathbb{R}$ and, as in previous sections, we take $p = \kappa\rho^\gamma$. The analytical problem consists of finding an appropriate spaces of functions such that if ρ_0 and u_0 are chosen from those spaces, then the solutions $\rho(x,t)$, $u(x,t)$ of (64) remain in those

spaces for all $t > 0$. We will not attempt a theoretical investigation of this problem here, but instead pursue a numerical treatment. In order to sidestep issues regarding the decay of solutions as $x \to \pm\infty$, we will take the domain U to be a compact interval $[0, L]$ equipped with the standard periodic boundary conditions (47).

We wish to test whether solutions of (64) approximate the shock wave solutions of the $1D$ barotropic compressible Euler equations. Of course, we already have evidence that this approximation is not going to be terribly good. From our results on traveling wave solutions, we know that there exists an initial condition u_0 (and an associated initial condition ρ_0) consisting of an upward-pointing pulse. This initial condition u_0 is rigidly transported to the right at a speed c by System S. No steepening, and indeed no change whatsoever in the shape of the wave occurs as it propagates.

This is already in sharp contrast with the solution of the $1D$ compressible Euler equation with the same initial data. In this case, the velocity field u would steepen and eventually form a shock wave at the point of inflection of u_0. At the instant at which this shock forms, the L^2 energy of the solution would drop. By comparison, the L^2 energy of the traveling wave solution stays constant for all time.

Description of the numerical method. We describe how to numerically solve System S (4a, 6) on the interval $[0, 1]$ with periodic boundary conditions. We use the barotropic law $p = \kappa\rho^\gamma$, with $\kappa = 0.4$, $\gamma = 1.4$. Pseudospectral techniques, as described in [10], play a large role in the method. First, we write the systems in semidiscrete form

$$\boldsymbol{\rho}_t = \mathbf{F}(\boldsymbol{\rho}, \mathbf{u}) \tag{65a}$$

$$\mathbf{u}_t = \mathbf{G}(\boldsymbol{\rho}, \mathbf{u}), \tag{65b}$$

where $\boldsymbol{\rho} = (\rho_1, \ldots, \rho_N)$ and $\mathbf{u} = (u_1, \ldots, u_N)$. Here, $\rho_i(t) \approx \rho(x_i, t)$ and $u_i(t) \approx u(x_i, t)$, where x_i, $i = 1, \ldots, N$, are grid points in the interval $[0, 1]$. We use the equispaced grid given by $x_i = (i - 1)\Delta x$ with $\Delta x = 1/N$.

The method carries the quantities $\boldsymbol{\rho}$ and $\mathbf{u}$ in physical space. We pass to Fourier space using the FFT only when we take derivatives. Before applying the inverse FFT to any quantity in Fourier space, we always use a two-thirds dealiasing rule. By this rule, the highest one-third wavenumber components of the spectrum are set to zero.

We see from (4a) that the ρ dynamics for System S is given by the standard continuity equation. Then, our function $\mathbf{F}(\boldsymbol{\rho}, \mathbf{u})$ is merely a pseudospectral approximation of the derivative $-(\rho u)_x$. In words, we first compute the product $(\boldsymbol{\rho}\mathbf{u})_i = \rho_i u_i$ and take the FFT of the result. After multiplying by $2\pi i\mathbf{k}$, where $\mathbf{k} = (-N/2 + 1, \ldots, N/2)$, and dealiasing, we take the inverse FFT, and multiply by -1.

Now we describe the construction of $\mathbf{G}$ for System S. Let us group all time-derivative terms from equation (6) in the following way:

$$\mathcal{A}u_t = -uu_x + \alpha^2\left(\frac{\rho_x}{\rho}uu_{xx} + u_x u_{xx} + uu_{xxx}\right) - \frac{p_x}{\rho}, \tag{66}$$

where $\mathcal{A} = \left[\mathrm{Id} - \alpha^2(\rho_x/\rho)\partial_x - \alpha^2\partial_{xx}\right]$. Again we use standard pseudospectral techniques to discretize and compute the right-hand side of (66); let us write the result of this as $\mathbf{b}$. To discretize the operator $\mathcal{A}$, we use standard high-order finite-difference approximations for ∂_x and ∂_{xx}. These approximations are, respectively (see [14,

Chap. 7.1]):

$$\mathcal{D}^1 = \frac{1}{\Delta x}\Gamma_0 \left[\mathrm{Id} - \frac{1}{6}\left(\Delta_0^2\right) + \frac{1}{30}\left(\Delta_0^2\right)^2\right] + \mathcal{O}(\Delta x^5) \tag{67}$$

$$\mathcal{D}^2 = \frac{1}{\Delta x^2}\left[\left(\Delta_0^2\right) - \frac{1}{12}\left(\Delta_0^2\right)^2 + \frac{1}{90}\left(\Delta_0^2\right)^3\right] + \mathcal{O}(\Delta x^6), \tag{68}$$

where Γ_0 and Δ_0^2 are operators on the space of vectors $\mathbf{z} = (z_1, \ldots, z_N)$, defined by

$$\left(\Delta_0^2 \mathbf{z}\right)_k = z_{k+1} - 2z_k + z_{k-1} \tag{69}$$

$$\left(\Gamma_0 \mathbf{z}\right)_k = \frac{1}{2}\left(z_{k+1} - z_{k-1}\right). \tag{70}$$

Because we impose periodic boundary conditions on the system, we use the convention that $z_k = z_{k+N}$ for all k. With this convention, the operators $\mathcal{D}^1$ and $\mathcal{D}^2$ can be written as matrices that include the periodic boundary conditions. We denote these matrices by D^1 and D^2, respectively.

Let $\mathbf{r}$ denote the result of computing ρ_x/ρ pseudospectrally. Now we are ready to write the discretization A of the operator $\mathcal{A}$:

$$A = \mathrm{Id} - \alpha^2 \,\mathrm{diag}(\mathbf{r}) D^1 - \alpha^2 D^2. \tag{71}$$

Here $\mathrm{diag}(\mathbf{r})$ is the diagonal matrix with $r_1, \ldots, r_N$ on the diagonal. We remark that the component-wise product of the vectors $\mathbf{r}$ and $\mathbf{z}$ can be written as the matrix-vector product $\mathrm{diag}(\mathbf{r})\mathbf{z}$.

Then the discretization of (66) becomes

$$A\mathbf{u}_t = \mathbf{b}, \tag{72}$$

which implies $\mathbf{G}(\boldsymbol{\rho}, \mathbf{u}) = A^{-1}\mathbf{b}$.

Having now described the construction of $\mathbf{F}$ and $\mathbf{G}$, we solve the ode system (65) with the fourth-order Runge-Kutta method. We remark that in practice, for System S, the presence of a third-derivative term on the right-hand side of (66) necessitates a CFL condition of $\Delta t \propto (\Delta x)^2$.

Numerical runs. Using the method just described, we performed numerical experiments for System S with the following initial conditions: the `gauss` data

$$\rho(x,0) = \frac{1}{100}\sin(2\pi x) + \frac{1}{2}, \tag{73a}$$

$$u(x,0) = \frac{1}{2}\exp(-25(x-1/2)^2), \tag{73b}$$

and the `sine` data

$$\rho(x,0) = \frac{1}{100}\sin(2\pi x) + \frac{1}{2}, \tag{74a}$$

$$u(x,0) = \frac{1}{2}\sin 2\pi x + \frac{3}{2}. \tag{74b}$$

We take $\alpha = 0.03$. We solve until $t = 5$ at resolution $N = 1024$. As the solutions evolved in time, we kept track of the energy (31) of the solution. All solutions presented in this work preserved their initial energy to within 0.1%. See Figure 3 for the solutions to System S for `gauss` and `sine` initial data. Movies of these solutions are available at

`http://www.cds.caltech.edu/~bhat/pub/.pde1/`

The important features of these numerical simulations are discussed in the next section.

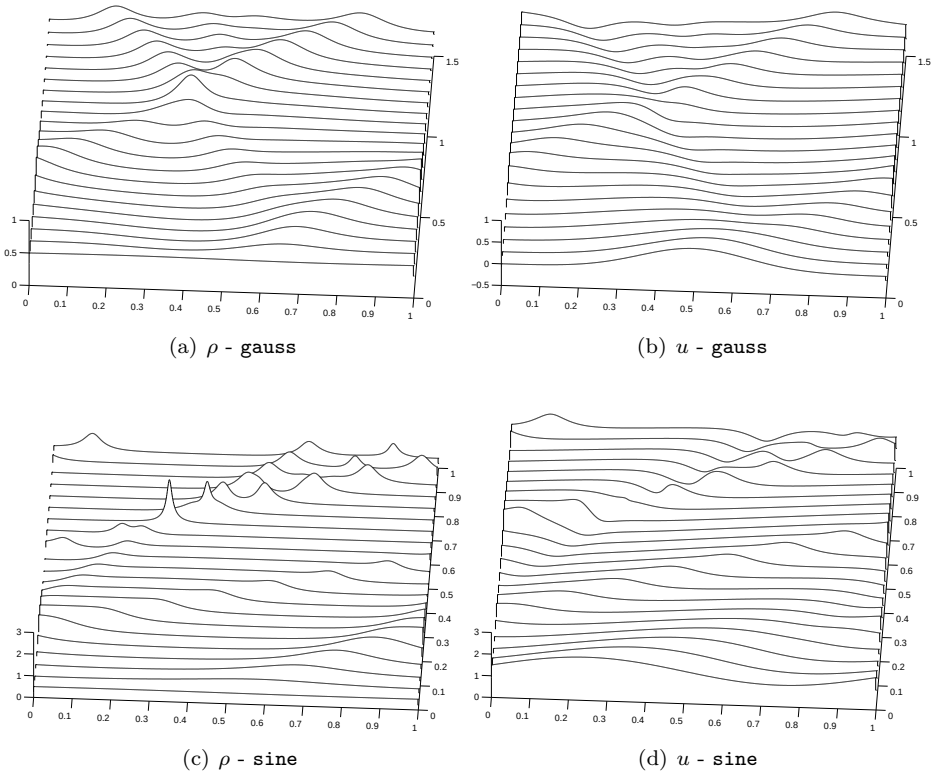

(a) ρ - `gauss` (b) u - `gauss`

(c) ρ - `sine` (d) u - `sine`

FIGURE 3. The solution of System S with `gauss` and `sine` initial data (73) and (74) , respectively. The figure shows the solution until $t = 1.5$ and $t = 1$, respectively. We performed runs until $t = 5$, and the solution manifests the same wave-like behavior, while preserving the energy h, given by (31), to within 0.1% of its initial value.

5. **Conclusions.** Unfortunately, our studies of the initial-value problem for System S indicate that it is not well-suited for the approximation of shock solutions of the compressible Euler equations. If one used either the `gauss` or `sine` initial conditions in the compressible Euler equations, the resulting solutions would contain shock waves at points of inflection of u. In all of our numerical experiments on System S, we have not seen any wave profiles that resemble smoothed or approximate shock waves.

For both ρ and u, the numerical solution retains its smoothness and stays bounded. Various wave-like structures of similar width appear and propagate to the right. Based on this and the fact that the energy stays very nearly constant, we conjecture that the systems are well-posed for sufficiently smooth initial data. However, analytic results on well-posedness need to be further investigated.

One way to approach the well-posedness issue is to attempt to use the geometric structure to one's advantage. Recall that the Lagrangian (3) for System S consists of kinetic minus potential energy. One can apply a Kaluza-Klein construction and turn this Lagrangian into a positive-definite metric on a certain enlarged space.

It would be of analytical interest to study the geodesic spray associated with this metric. For one, it may yield a new method of proving existence/uniqueness for regularized gas dynamical equations.

We note that especially in the evolution of $\rho(x,t)$ given the `sine` initial data, we see the emergence of numerous symmetric patterns and oscillations that hint at deep, fundamental structures for System S. This includes geometric structures such as higher-order symmetries for System S that are waiting to be discovered, as well as algebraic structures related to complete integrability. System S already has one Hamiltonian structure, the semidirect product Euler-Poincaré structure mentioned above (see (31)). If System S possessed another compatible Hamilonian structure, then it would be completely integrable in the sense of Lax.

Indeed, it would be interesting to apply a Painlevé test to System S to determine whether it is completely integrable. We may also study the relationship between System S and a completely integrable hierarchy of equations derived from the barotropic Euler equations by [4].

Finally, the stability of the traveling wave solutions of System S is an important question that we will address in future work. Here the geometric structure of the problem will be quite useful—we hope to obtain a stability result by applying the energy-Casimir method as described in [17].

Acknowledgments. The authors would like to thank Jerry Marsden, Darryl Holm and Joe Keller for helpful comments regarding this work. We would also like to thank Kamran Mohseni for pointing out the Favré averaging technique, and Matt West for suggesting the "filtering" style derivation of the compressible averaged equations. Harish S. Bhat acknowledges support from a National Science Foundation Graduate Research Fellowship.

REFERENCES.

[1] R. Abraham, J. E. Marsden and T. S. Ratiu, Manifolds, tensor analysis, and applications, volume 75 of *Applied Mathematical Sciences*, Springer-Verlag, New York, 2004, Draft edition.

[2] H. Bhat, R. C. Fetecau, J. E. Marsden, K. Mohseni and M. West, Lagrangian averaging for compressible fluids. *SIAM J. Multiscale Modeling and Simulation*, **3** (2005),818 – 837.

[3] G. Birkhoff and G.-C. Rota, Ordinary differential equations, Blaisdell, Waltham, MA, second edition, 1969.

[4] J. C. Brunelli and A. Das, On an integrable hierarchy derived from the isentropic gas dynamics, *J. Math. Phys.*, **45** (2004), 2633–2645.

[5] R. Camassa and D. D. Holm, An integrable shallow water equation with peaked solitons, *Phys. Rev. Lett.*, **71** (1993), 1661–1664.

[6] S. Y. Chen, D. D. Holm, L. G. Margolin and R. Zhang, Direct numerical simulation of the Navier-Stokes alpha model, *Phys. D*, **133** (1999), 66–83.

[7] P. Deift, S. Venakides and X. Zhou, An extension of the steepest descent method for Riemann-Hilbert problems: The small dispersion limit of the Korteweg-de Vries (KdV) equation, *Proc. Nat. Acad. Sci*, **95** (1998), 450–454.

[8] A. Favre, Équations des gaz turbulents compressibles I, *J. Méc.*, **4** (1965), 361–390.

[9] C. Foias, D. D. Holm and E. S. Titi, The three dimensional viscous Camassa-Holm equations and their relation to the navier-stokes equations and turbulence theory, *J. Dynam. Differential Equations*, **14** (2002), 1–36.

[10] B. Fornberg, A practical guide to pseudospectral methods, volume 1 of *Cambridge monographs on applied and computational mathematics*, Cambridge University Press, New York, 1996.

[11] D. D. Holm, Fluctuation effects on 3D Lagrangian mean and Eulerian mean fluid motion, *Physica D*, **133** (1999), 215–269.

[12] D. D. Holm, J. E. Marsden and T. S. Ratiu, The Euler-Poincaré equations and semidirect products with applications to continuum theories, *Adv. Math.*, **137** (1998), 1–81.

[13] D. D. Holm, J. E. Marsden and T.S. Ratiu, Euler-Poincaré models of ideal fluids with nonlinear dispersion, *Phys. Rev. Lett.*, **349** (1998), 4173–4177.

[14] A. Iserles, A first course in the numerical analysis of differential equations, Cambridge University Press, New York, 1996.

[15] S. Kamvissis, K. D. T.-R. McLaughlin and P. D. Miller, *Semiclassical soliton ensembles for the focusing nonlinear Schrödinger equation*, volume 154 of *Annals of Mathematics Studies*, Princeton University Press, Princeton, NJ, 2003.

[16] P. D. Lax and C. D. Levermore, The small dispersion limit of the Korteweg-de Vries equation, *Comm. Pure Appl. Math.*, **36** (1983), I 253–290, II 571–593, III 809–829.

[17] J. E. Marsden and T. S. Ratiu, Introduction to mechanics and symmetry, volume 17 of *Texts in Applied Mathematics*, Springer-Verlag, New York, second edition, 1999.

[18] J. E. Marsden, T. S. Ratiu and A. Weinstein, Semidirect products and reduction in mechanics, *Trans. Amer. Math. Soc.*, **281** (1984), 147–177.

[19] J. E. Marsden and S. Shkoller, Global well-posedness for the lans-α equations on bounded domains, *R. Soc. London Philos. Trans. Ser. A Math. Phys. Eng. Sci.*, **359** (2001), 1449–1468.

[20] K. Mohseni, B. Kosović, S. Shkoller and J. E. Marsden, Numerical simulations of the Lagrangian averaged Navier-Stokes equations for homogeneous isotropic turbulence, *Phys. Fluids*, **15** (2003), 524–544.

[21] C. G. Speziale, G. Erlebacher, T. A. Zang and M. Y. Hussaini, The subgrid-scale modeling of compressible turbulence, *Phys. Fluids*, **31** (1988), 940–942.

[22] A. Tovbis, S. Venakides and X. Zhou, On semiclassical (zero dispersion limit) solutions of the focusing nonlinear Schrodinger equation, *Comm. Pure Appl. Math.*, **57** (2004), 877–985.

[23] W. G. Vincenti and C. H. Kruger, Introduction to physical gas dynamics, Wiley, New York, 1965.

[24] G. B. Whitham, Linear and Nonlinear Waves, Wiley-Interscience, New York, 1974.

Received June 2005; revised March 2006.

E-mail address: hsb2106@columbia.edu
E-mail address: van@math.stanford.edu